AD-A121 817 DISEASE MODELLING OF JAPANESE ENCEPHALITIS IN TAIWAN THROUGH THE USE OF SATELLITE REMOTE SENSING(U) EARTH SATELLITE CORP CHEVY CHASE MD C SHEFFIELD 30 AUG 82 1/1

UNCLASSIFIED N00014-81-C-0712 F/G 6/5 NL

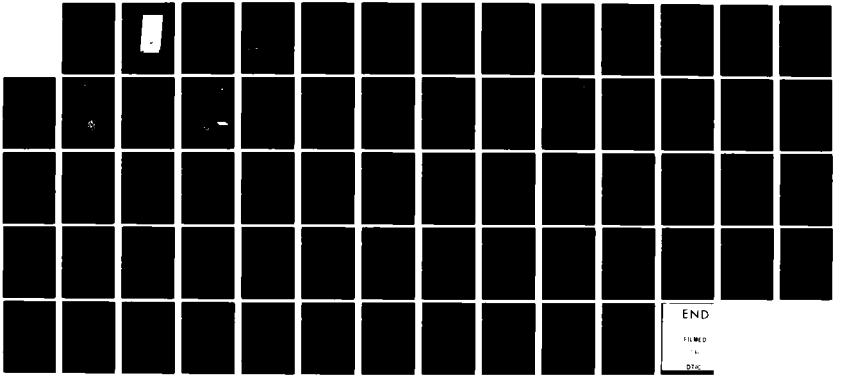

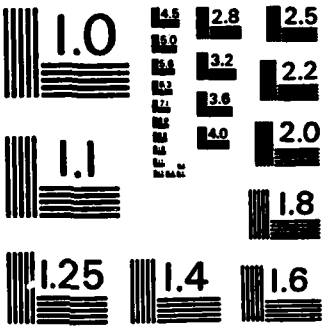

MICROCOPY RESOLUTION TEST CHART
NATIONAL BUREAU OF STANDARDS - 1963 - A

DISEASE MODELLING OF JAPANESE ENCEPHALITIS IN TAIWAN THROUGH THE USE OF SATELLITE REMOTE SENSING

Prepared for
THE NAVAL MEDICAL RESEARCH INSTITUT
U.S. NATIONAL NAVAL MEDICAL CENTER
Under Contract N00014-81-C-0712

August 30, 1982

EARTH SATELLITE CORPORATION *(EarthSat)*
Chevy Chase, Maryland, USA

TECHNICAL REPORT STANDARD TITLE PAGE

1. Report No.	2. Government Accession No.	3. Recipient's Catalog No.
	AD-A121 817	

4. Title and Subtitle	5. Report Date
Disease Modelling of Japanese Encephalitis in Taiwan Through the Use of Satellite Remote Sensing	August 30, 1982
	6. Performing Organization Code
7. Author(s)	8. Performing Organization Report No.
Charles Sheffield	
9. Performing Organization Name and Address	10. Work Unit No.
Earth Satellite Corporation 7222 47th Street Chevy Chase, Maryland 20815	11. Contract or Grant No. N00014-81-C-0712
	13. Type of Report and Period Covered Final Report September 1981 - September 1982
12. Sponsoring Agency Name and Address	14. Sponsoring Agency Code
Naval Medical Research Institute National Naval Medical Center Bethesda, Maryland 20014	

15. Supplementary Notes

16. Abstract

This report describes the development of probability models for the occurrence of infectious disease using variables derived from the Landsat series of satellites and other geographic factors. The models are applied to yield a predictive program for the occurrence of Japanese encephalitis on the island of Taiwan. Four different forms of model are evaluated: linear regression, log-linear regression, logit models, and discriminant analysis. Observations consisted of disease data from 106 sites in Taiwan, in the period 1968-1975. Of the models employed, it was found that linear regression produces the best results, and a 9-variable linear regression was preferred. The independent variables in this case consist of means and variances of Landsat data over regions surrounding each disease site, plus altitude data. A significant correlation was found between observed and predicted disease incidence rates (correlation coefficient = 0.75). No systematic residual biases were observed in the final predicted results. The overall form of the model and the use of the data should remain the same for many infectious diseases in many different parts of the world.

17. Key Words (Selected by Author(s))	18. Distribution Statement
Japanese encephalitis, Landsat, infectious disease, statistical model, remote sensing, Taiwan.	

19. Security Classif. (of this report)	20. Security Classif. (of this page)	21. No. of Pages	22. Price*
Unclassified	Unclassified	60	

*For sale by the Clearinghouse for Federal Scientific and Technical Information, Springfield, Virginia 22151.

FOREWORD AND ACKNOWLEDGEMENTS

This study is the product of a contract (N00014-81-C-0712) funded by the Office of Naval Research as part of a Naval Medical Research and Development Command DD 1498 number MF58524.009 entitled "Infectious Diseases Risk Assessment in Foreign Operations Involving Military Forces." The Principal Investigator of this work unit is LT Gary Pazzaglia and the Associate Investigator is Ms. Eleanor Cross. We wish to express thanks to LCDR James Olson of the Yale Arbovirus Research Unit for supplying the required disease data for Japanese B encephalitis in Taiwan and to Dr. Charles Barnes of the International Veterinary Medical Foundation for helping to formulate the conceptual framework for this study. Appreciation is also given to CDR R. I. Walker of Naval Medical Research Institute for guidance in overall project design.

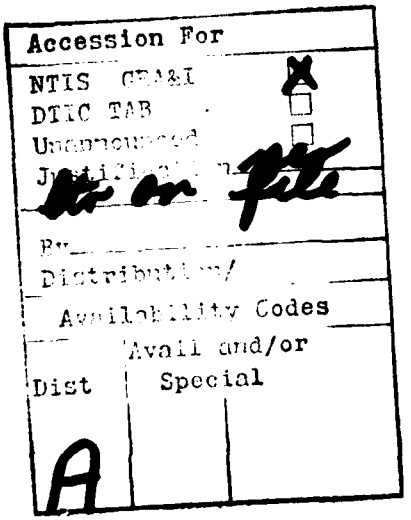

GENERAL SUMMARY

Military operations frequently require the introduction of non-indigenous personnel to geographic areas for which data on infectious diseases are absent or unreliable. For many parts of the world, prior ground or aircraft reconnaissance may also be impossible.

This report addresses the problem of assessing the probability of infectious disease occurrence using generally available geographic variables. In particular, variables are employed that utilize data provided by the Landsat series of satellites, combined with altitude and location information. A set of statistical models is developed and applied to the analysis of a particular disease, that of Japanese encephalitis occurring on the island of Taiwan.

Following a description of the general characteristics of data provided by the Landsat satellites, a summary of relevant facts concerning the etiology of Japanese encephalitis is presented. These facts dictate the general form of statistical models to be employed in numerical experiments. Four models are applied: linear regression, log-linear regression, logit models, and discriminant analyses. In each case, observed disease data for a set of 106 sites in Taiwan for the period 1968 to 1975 constitute the dependent variables, with independent variables obtained from Landsat, altitude and location data.

Of the four models employed, it is found that linear regression analysis offers the most promise. Within the set of linear regression models employed, a 9-variable form gives the best results. The independent variables in this

preferred case consist of altitudes of disease sites and the means and variances of Landsat data over square regions surrounding each disease site location.

Use of this model over sets of Taiwan disease sites leads to a significant correlation between observed and predicted incidence rates for Japanese encephalitis. The observed correlation coefficient of 0.75 is insensitive to the particular subset of disease sites used to develop the model coefficients, and no systematic biases are discernible in the final predicted results. The etiology of the disease suggests that the future inclusion of additional independent variables, in particular weather variables, might strengthen the correlations.

The results of this work consist of a set of statistical models whose coefficents must be determined for any particular disease and geographic region. However, the overall form of the model and the use of data should remain the same for many infectious diseases, in many different parts of the world.

TABLE OF CONTENTS

DISEASE MODELLING OF JAPANESE ENCEPHALITIS IN TAIWAN THROUGH THE USE OF SATELLITE REMOTE SENSING

I. INTRODUCTION

Attempts to understand the occurrence and spread of infectious diseases probably pre-date written history, although scientific ideas on the subject are of much more recent vintage. The notion of bacterial action as an immediate physical cause of disease was proposed by Girolamo Fracastoro more than four hundred years ago, in 1546,[1] but its acceptance awaited Pasteur's and Koch's work in the 1870's.[2,3] The idea that insects might serve as vectors for disease transmission is more recent yet, dating only from Smith and Reed's work[4,5] at the end of the last century.

Although there still remain large gaps in our understanding of the detailed interactions between hosts and vectors as they govern the occurrence and propagation of arthropod-borne diseases, we can now feel confident that the following factors are all of great significance in determining the probability of infection and spread of human disease:

- the sensitivity of both host and vector to climatic and geographic variations, including habitat, temperature, altitude, landforms, and rainfall;
- the presence or absence of alternate animal hosts that serve as potential amplifiers for disease occurrence (as, for example, hogs serve as an amplifying factor for Japanese encephalitis);
- the distribution and degree of exposure of the human population;
- the innate or induced resistance of the human population;
- the prevailing regional cultural practices, e.g., cleanliness and sanitation.

When, as is frequently the case in military operations, a group of non-indigenous humans is introduced to a region, data on disease occurrence will often be lacking. The native populations may possess acquired immunity, or the region may be so sparsely populated that data on diseases are non-existent, or lack any statistical validity. In many parts of the world, inadequate reporting systems for disease data are the rule rather than the exception. There is a definite need for some predictive tool which can take detailed geographic knowledge of a region and make reasonable estimates as to the disease rates that would be encountered in a non-immune group entering the region.

The biggest impediment to the use of predictive models based on fundamental biological interactions is the absence of knowledge of explicit causal relationships. The physical variables that couple environment, human host, vector and disease agent are frequently unknown in the necessary detail. However, in such circumstances, it is always possible to employ a purely statistical model in which relationships are studied empirically and through statistical correlations. No predictor of this type will offer perfect performance, and there will remain unknown influencing factors. In addition, it will normally require more data to establish the parameters of a statistical model than a biologically defined model, since the functional form of the latter is known from the biology, whereas the former must rely on the data to define both the form and the unknown constants of the model. On the positive side, an established statistical correlation can often suggest a productive approach to deterministic models based more on causal relationships.

All statistical models are inherently data dependent. Thus in military operations a further complication arises when areas are inaccessible to ground investigation or to aircraft overflight. In practice, these areas may also be those of greatest military interest.

In such circumstances, data acquired remotely by artificial satellites can often provide the detailed overview needed for disease distribution models, defining the necessary land use, geography, ground cover and topography. Such data can be obtained regularly throughout the year, without a ground or aircraft presence, and represent a powerful new potential for disease distribution modelling.

In this report, the first steps are taken towards a distribution model for infectious diseases that is minimally dependent on ground presence or aircraft overflights. The first application has been to a particular disease in a particular location (Japanese encephalitis on the island of Taiwan) but the principles employed are quite general, and the supporting satellite data base is available anywhere in the world.

The organization of the report is as follows:

Section I - Introduction: Background on the modelling of infectious diseases, and the governing variables that apply.

Section II - Remote sensing and the information provided by satellite coverage: An overview of the Landsat program and the data provided by it.

Section III - Japanese encephalitis and its suitability to distribution modelling: A summary of studies performed to date of the disease and the factors that appear relevant to its propagation.

II. REMOTE SENSING AND THE INFORMATION PROVIDED BY SATELLITE COVERAGE

A. The uses of remote sensing and the U.S. Earth Resources Program

The idea that information useful for natural science investigations might be obtained from satellites arose as a natural extension of the use of aerial photographs in the first half of this century. Early experiments using balloon-borne cameras for monochrome photography in the 1850's[6] led to the use of aerial photography for survey purposes in the 1920's[7]. In the Second World War, the power of infrared film to distinguish camouflage from healthy growing vegetation began the use of wavelengths beyond the visible,[8] and in the 1960's handheld cameras aboard the Gemini and Apollo spacecraft showed the power of photographic coverage of a very large area.

It was therefore natural, when a series of satellites for the measurement of the Earth's resources was conceived in the late 1960's, that multiple uses of the data would be attempted. The initial list of roughly 350 experiments approved by NASA in 1972 for the first such satellite (known originally as ERTS-1 and later as Landsat-1) covered numerous disciplines and application areas.[9] These ranged from practical applications in crop monitoring, geological mapping, and oil and gas exploration, to experiments aimed at determining the best manner of presenting the information collected by the spacecraft. There were even experiments performed for disease monitoring, but they were confined to timber disease, where the effects on growing trees were directly visible on the images. No experiments for the use of satellite data for human disease distribution were proposed, perhaps because of the lack of explicit causal models that could link observable ground features with disease incidences. However, soon after the launch of Landsat-1, satellite data from the NOAA 2 and NOAA 3 satellites were used successfully in the U.S./Mexico Screwworm Eradication

Project in 1973-1975.[10]

The satellites of the U.S. Earth Resources Program were not designed for high-resolution surveillance work, and in fact all the data collected by the program is unclassified and can be purchased for use by anyone. As a result, there are practical limitations on the smallest size area that can be analyzed using such data; as a compensating advantage, very large areas (more than ten thousand square miles) can be analyzed in a single image.

In addition to the Landsat satellites that provided the main data source for this project, the United States operates weather service satellites that give worldwide coverage at visible and thermal infrared wavelengths several times a day. These satellites offer a less detailed picture than the Landsat satellites, but have the advantage of more frequent coverage of any particular ground area.

B. The Landsat system

Four Landsat spacecraft have so far been launched, but data from Landsat-4 (launched July 1982) are not yet available. Landsats-1, -2 and -3 move in sun-synchronous orbits so that each satellite images the Earth at the same local time of day, about 9:30 a.m. The orbits are close to polar, almost circular, and have a period of 103 minutes. The satellites travel at an average height of about 900 kilometers, and each satellite provides complete coverage of the Earth's surface in latitudes lower than 81° every 18 days[11] (Figure 1). Landsat-4 occupies a lower orbit with an average height of about 700 kilometers and provides complete coverage of latitudes lower than 81° every 16 days.

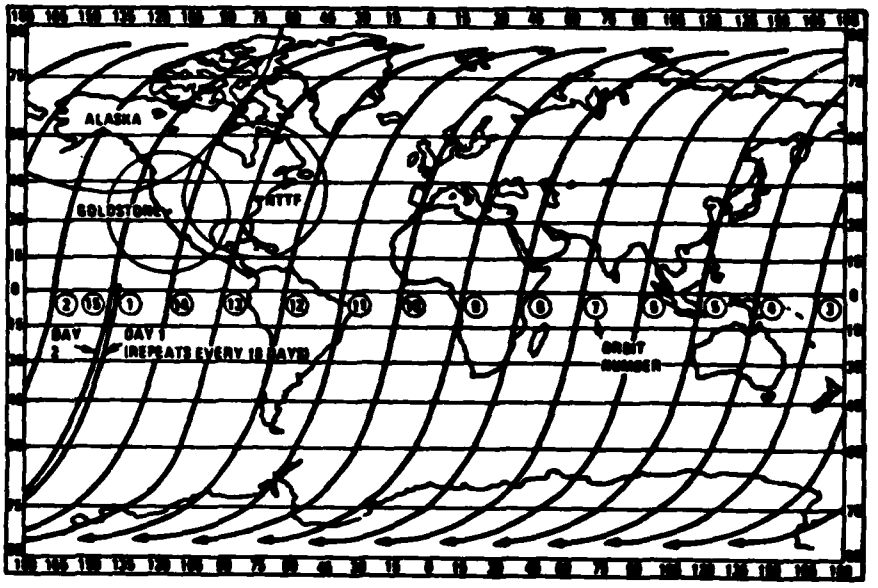

Typical Landsat ground trace for one day;
only southbound passes shown
(modified from NASA).

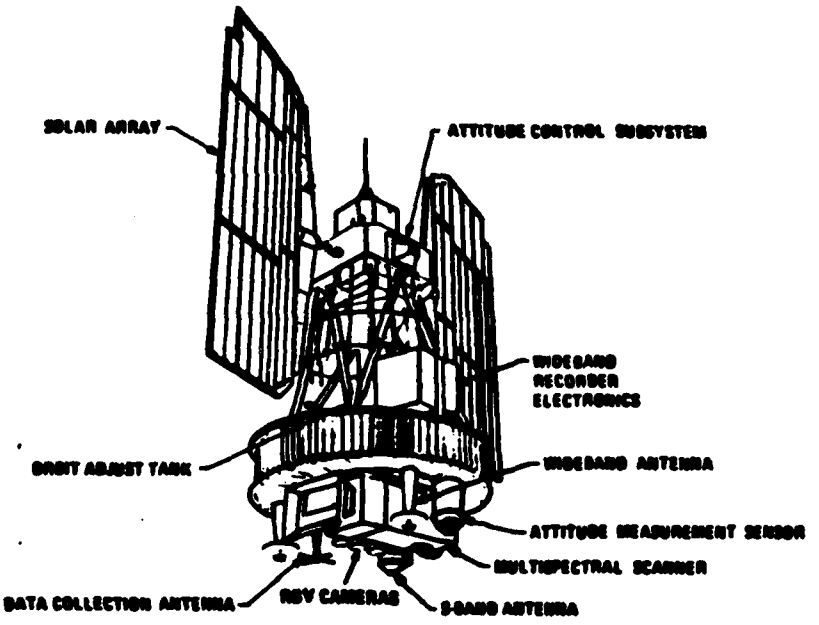

Figure 1. The Landsat Satellite (modified from NASA).

Cloud cover may diminish the usefulness of acquired data since the sensing of the Earth's surface takes place only in visible and near-visible wavelengths which have no cloud penetrating power. This can be a severe drawback in equatorial regions, where cloud cover is present most of the time.

The primary observing instrument on the first three Landsat spacecraft, and the one that was used to provide data for this project, is a Multi-Spectral Scanner (MSS). It senses reflected radiation from the Earth with a field of view that covers an area 79x79 metres on the Earth's surface. The incident radiation at the spacecraft is spectrally decomposed in the spacecraft optics to four wavelength regions: 0.5 to 0.6 micrometres (usually termed the "green band"); 0.6 to 0.7 (the "red band"); 0.7 to 0.8 (the "first infrared band"); and 0.8 to 1.1 (the "second infrared band"). Successive scan lines of data are generated by the forward motion of the spacecraft in its orbit. A complete coverage of a swath of the surface, roughly 185 kilometres wide, is continuously generated as the spacecraft traverses the daylight side of the Earth. (Note: The fourth spacecraft in the series, Landsat-4 has a thermal infrared band that permits night-side sensing also; a similar instrument on Landsat-3 never returned usable data because of detector malfunction.)

The four spectral bands of data are returned to Earth in two separate modes. If the spacecraft is in line-of-sight range of a Landsat ground receiving station, the data are converted to digital form and transmitted electronically in real-time to the station. If no station is in line-of-sight range, data may be stored on on-board tape recorders, for subsequent electronic transmission to a ground station (See Figure 2). During the process of transmission to the ground, the signal in each spectral band is

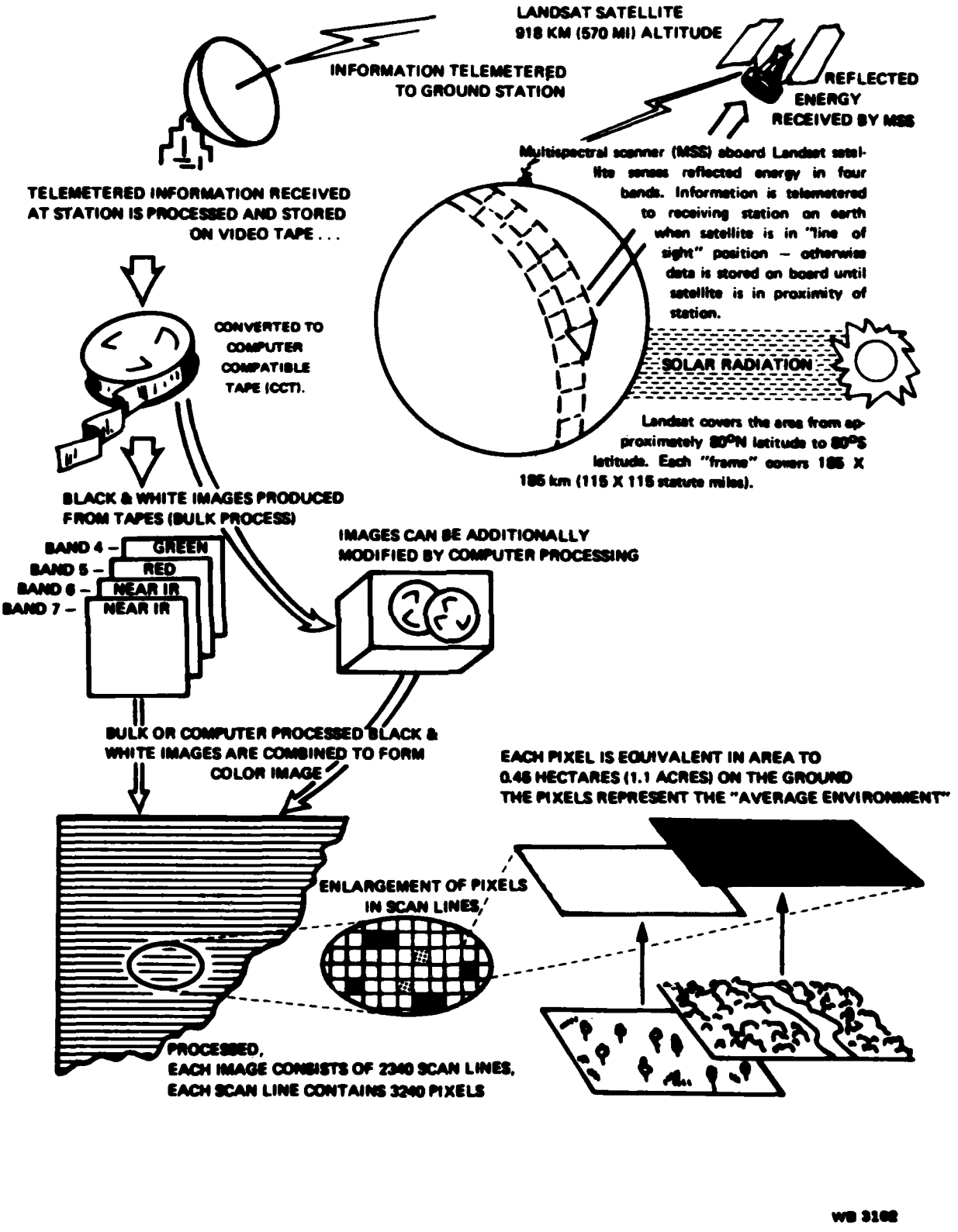

Figure 2. Sequence of Landsat Information System

over-sampled to give a ground resolution along the scan-line of 57 metres. Thus the received digital signal is that of sets of ground areas each 79m x 57m, roughly 1.1 acres, in each of four spectral bands. The digital signal returned to Earth from the satellite assigns the observed ground reflectances to one of 64 distinct reflectance levels (256 for Landsat-4) that are usually termed grey levels. The individual distinguishable ground areas are termed picture elements, or pixels.

Although the observations made by the scanner are a continuous swath of data of width 185 kms, for practical use the data stream is arbitrarily chopped into sections corresponding to squares of 185 km^2. This is conventionally termed a Landsat "scene" or "frame." Each such frame contains roughly 7.6 million pixels. The very large volumes of data that constitute a single Landsat scene make computer processing mandatory.

Before the information provided by the spacecraft can be used, a number of geometric and radiometric corrections must be applied. The most obvious one in terms of the appearance of the reconstructed image is the correction for Earth rotation, which leads to a rhomboidal rather than a square shape for a single image frame. However, for practical use of the data, the most important correction is probably that compensating for variations in detector sensitivity, which if it occurs, leads to a striped or banded image and strongly degrades the spectral fidelity of the data. This is a very important factor in activities such as image classification, or in the statistical analyses performed on this project.

Landsat data are typically displayed in a standard false color presentation in which the first infrared band (0.7 to 8.0μm) is not used. This

is usually justified since there are strong correlations between the data of the first and second infrared band. However, in this work all possible statistical strength was desirable, and all experiments employed all four Landsat spectral bands.

III. JAPANESE ENCEPHALITIS AND ITS SUITABILITY TO DISTRIBUTION MODELLING

A. History and etiology of Japanese encephalitis

The disease now recognized as Japanese encephalitis (JE) and also as "summer encephalitis" occurs throughout eastern Asia, as far north as Siberia and as far south as the East Indies from Guam to eastern India. The disease is characterized by fever, encephalitic symptoms, and a high mortality rate. It attacks primarily young children during the summer season. The incidence of the disease correlates with the warm part of the year in areas to the north of Taiwan, including Okinawa and Japan, and shows much less correlation with season south of Taiwan.[12] Japanese encephalitis was first reported in Taiwan by Sakai in 1935, and has been a legally defined reportable disease by the Taiwan Provincial Health Department since 1955.[13]

The primary vector for the transmission of JE virus on Taiwan is Culex tritaeniorhynchus, with C. fuscocephalus as a possible other vector in the southern part of the island.[14] C. tritaeniorhynchus is a mosquito that breeds in clean water in cultivated fields, and in stable bodies of water around such fields.[15] There is a rapid seasonal increase in the population of the mosquito, with a peak in July and August, that may be linked to some specific agricultural practice on the island. However, in India and in Thailand there is some evidence that the population of the adult mosquito may be more influenced by rainfall rather than any type of irrigation practice.[16] In more northern areas, including Taiwan, mosquito population densities seem to follow the annual temperature curves, with peak adult population in the summer months.

The disease rates for a human population newly introduced to Taiwan would probably be quite different from the native population, since they would

lack any previous exposure to the JE virus. It appears that a large percentage of the adult native population is immune as a result of childhood infection, often of a subclinical nature.[13] Nonetheless, JE was one of the most important endemic diseases of the island during the period studied. The development of a suitable JE vaccine and its use from 1976 onwards in a successful public health program have in recent years much reduced the prevalence of the disease.

Of the facts cited here, the ones that are of the most significance in establishing a disease distribution model are thought to be as follows:

1. The definition of JE as a legally reportable disease has produced reliable disease statistics for Taiwan. There is a data base that gives not only incidence rates, but the specific place of residence associated with each case. This is unusual, since disease data are commonly aggregated to the point where specific geographic locations disappear. Since we are seeking to correlate the disease with site-specific geographic variables, site-specific incidence rates are essential.

2. The vector for JE breeds in particular environments that should be correlatable with land cover and land use discernible from space imagery.

3. The probable presence of alternate hosts, in particular the domestic swine, complicates the analysis. Disease foci may be expected around hog farms, which may or may not be distinguishable with the resolution of the data provided by the Landsat satellites.

4. Prior infection of the native population will reduce current disease levels; thus disease incidence rates may reflect stability of population at one location as much as they indicate the exposure risk at that location.

B. Japanese encephalitis data for Taiwan

Disease incidence rates for JE in Taiwan were collected by the Taiwan Provincial Health Department at 106 locations, mainly in the western part of the island in the period 1968-75. Figure 3 shows the locations of cases occurring during 1968-69 and is representative of the geographic distribution of all cases over the entire study period. For each site, the name of the location, its latitude and longitude, the population estimate for 1980, and the disease incidence rate per 100,000 were determined. Close examination of 1:50,000 scale base maps of Taiwan revealed that the cited latitudes and longitudes for the towns and villages were only approximate, therefore more accurate locations were taken from the maps. The original data are shown in Appendix A. Note that the data include cases where no disease was reported, which is important information when we wish to discriminate between different areas for the purpose of disease occurrence probabilities.

Each reported site corresponds to a town or village, and the examination of Landsat images of Taiwan makes it clear that these villages are of variable geographic size. The table in Appendix A also shows that we are dealing with widely varying populations associated with different disease sites. This point is important, since population density is probably a significant factor in disease propagation, independent of geographic or climatic considerations.

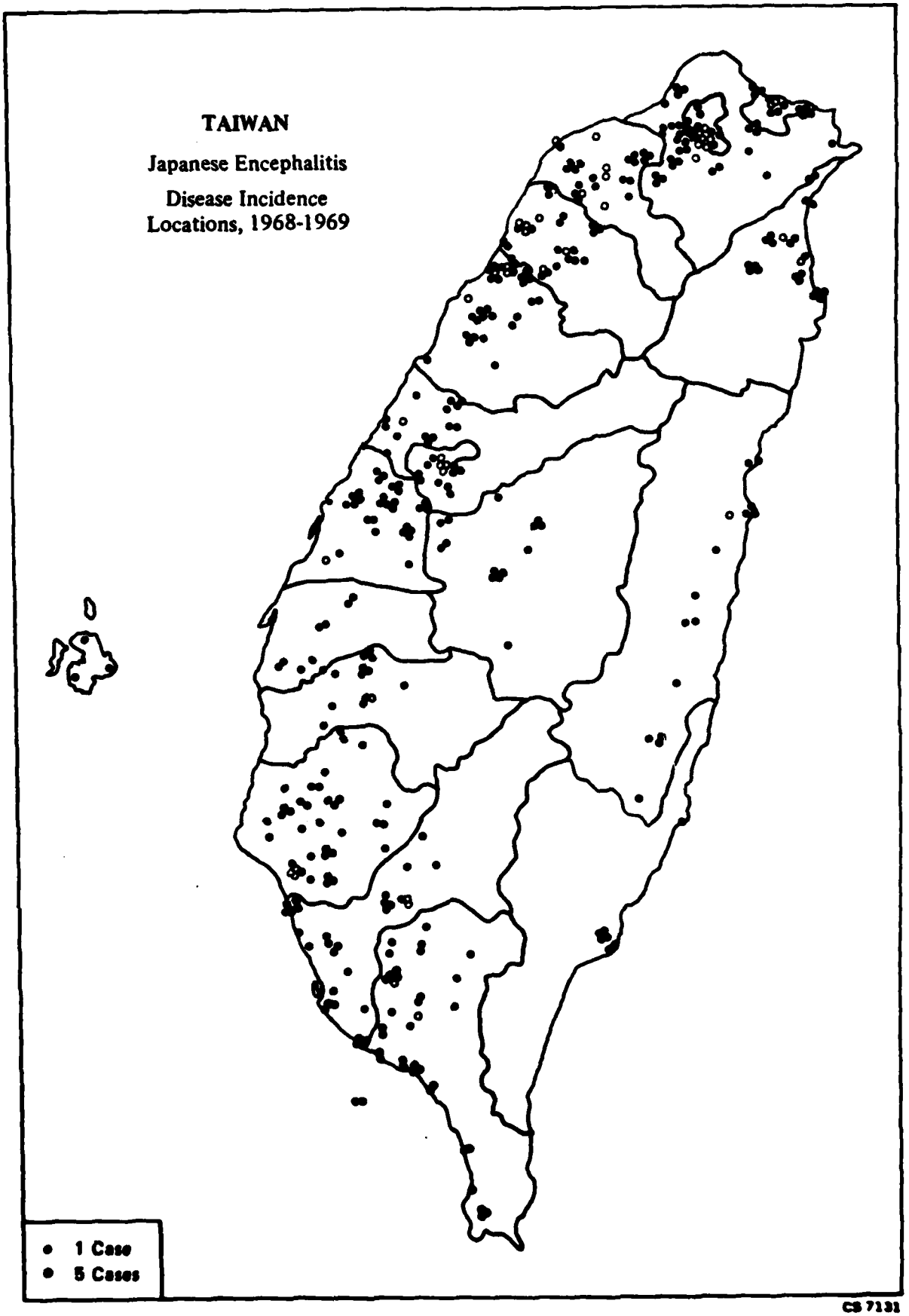
TAIWAN
Japanese Encephalitis
Disease Incidence
Locations, 1968-1969
1 Case
5 Cases
CS 7131

Figure 3.

The disease incidence data, populations, and locations were used to create a computer data file for subsequent statistical analysis in the disease distribution models. No grouping was performed, therefore each location and disease incidence rate is treated as a single, independent observation in the models. Since there is also no *a priori* reason to believe that any observation is more reliable than any other, equal data weights were assigned to each observation.

IV. THE STATISTICAL MODELS EMPLOYED IN THE INVESTIGATION

A. Selection of models

The base assumptions underlying the choice of statistical models in the project can be summarized as follows:

1. The spatial distribution of JE on Taiwan is not determined by a strictly random process. It is primarily the result of the simultaneous occurrence of a number of events and conditions, each of which must be present in some measure before Japanese encephalitis can result. Correlations between disease occurrence and other physical variables must therefore exist and should be susceptible to analysis.

2. Although the occurrence and spread of JE in Taiwan is not the result of purely chance happenings, random processes, or ones that appear random in any macroscopic analysis of the disease, will also play a part. Any model that is used can therefore be expected to display significant variation between observed and predicted values.

3. There exist environmental markers that are closely associated with the causal factors that determine the distribution of the disease. Even when there is no direct causal link with geographic and climatic variables, there will probably exist indirect coupling capable of statistical analysis.

4. There is no *a priori* reason to prefer a particular form of relationship between the dependent and the independent variables; thus a postulated linear relationship is an acceptable starting point for investigation.

5. The number of cases of disease per 100,000 of population is small (less than 100); therefore although the incidence rate per 100,000 could theoretically range from 0 to 100,000, in practice we can safely use a model that assumes observed and predicted rates must remain small.

Given these initial assumptions, the statistical techniques selected for use on the project were as follows. Each technique is described in more detail following this initial summary.

1. Regression analysis,[17] with the observed disease incidence rates as dependent variable, and derived properties of Landsat data and topographic data as independent variables. The particular Landsat-derived variables will be described in Section V; here, it will only be noted that we were using between 4 and 15 independent variables in the model.

The principal virtue of linear regression models is simplicity. The principal disadvantage, at least in this application, is that predicted values can take on any value, including negative values. Since a negative disease incidence rate is meaningless, a model that is constrained to yield only positive or zero values for the dependent variable is clearly preferable.

Normality of the dependent variable is also assumed in regression methods. In the present instance, possible departures from normality are probably not a significant factor, since they are likely to be outweighed by model deficiencies.

2. Logit models,[19] again with the observed disease incidence rates as dependent variable and the derived properties of Landsat data and topographic data as independent variables.

The principal virtues of the logit models are their robustness and the fact that they deal in probablities. They are non-parametric, and they also guarantee that predicted disease incidence rates cannot be negative (since probabilities must lie between zero and one).

The principal disadvantage of the logit models is their complexity, since they are inherently nonlinear and must be iterated to some converged solution. They also appear to work less well when all the probabilities involved lie very close to zero. Since in the case of the JE data the rates per head of population are always far less than one, and since it is these rates that are treated as probabilities within the logit models, they are not ideal for the present application.

3. Discriminant analysis,[18] in which the observed disease incidence rates are used to classify Landsat data and topographic data into a set of discrete incidence rate classes. Discriminant analysis techniques have the advantage that they apply to cases where the dependent variable is a non-numerical entity; thus by dichotomizing the dependent variable into disease incidence ranges, any problems with negative disease incidence predictions can be avoided.

The main disadvantage with discriminant analysis is the loss of a precise numerical result. Used predictively, the methods will assign any new geographic area to a class (which will in this case be a range of levels of disease incidence), but the methods do not predict a precise numerical value. In addition, it frequently happens that new data points cannot reasonably be assigned to any existing class, i.e., they statistically belong to a disease incidence rate not included in the original model. This is similar to the problem with regression models, which may assign a predicted numerical value for disease incidence that appears either negative or impossibly high. In both cases, what we are seeing is a failure either of the model employed, or of the ability of the given data to establish the model's parameters.

Another common finding that again describes a weakness either of the model or of the data available is an inability of the discriminant classifier to resolve the data set into any "clean" classes without a high degree of overlap. If the initial data do not define a separable group of classes, assignment of any new data to a class is suspect. Strongly overlapping classes are frequently handled in practice by collapsing them to form a single new class, but this often leads to a final classification with too few classes to be useful in the prediction process.

Discriminant analysis methods have been used very widely with Landsat data, mainly for the purposes of crop classification.[20] The approach to classification using Landsat is discussed further in Section IV.D.

B. *The regression analysis model*

A linear multiple regression model with unit data weights was employed on the project, of the form:

Disease occurrence at site k (k = 1 to K)

$$D(k) = \sum_{n=1}^{N} \alpha(n).L(n,k) \qquad \text{------(1)}$$

In this expression, N is the number of parameters in the model, the coefficients $\alpha(n)$ are constants to be determined from the data, and the values L(n,k) are functions of the Landsat data and other geographic variables associated with the individual disease occurrence sites as will be described in Section V.

In applying the regression model, the data set is divided into two parts, a "training set," and a "test set." Model coefficients developed using only the training set data are then used to predict the disease incidence rates for the test set.

The principal measure of goodness of fit is the normalized sum of squares of the residuals,

$$R = \sum_{k=1}^{K} (D(k)^{\text{observed}} - D(k)^{\text{computed}})^2/(K-N-1) \qquad \text{------(2)}$$

The model can be used with any number of coefficients less than or equal to the number of data points, up to a maximum of 20 coefficients.

A variant on this model, in which the logarithm of disease incidence rates is used in place of the rates themselves, is also available. Such a model assures that the predicted disease incidence rates are always positive,

since when the logarithm of disease rate extends over the range from $-\infty$ to $+\infty$, the disease rate itself goes from 0 to $+\infty$.

This log-linear regression model has the form:

$$\log D(k) = \sum_{n} \alpha(n).L(n,k) \qquad \text{------(3)}$$

Use of the log-linear model to determine the regression coefficients abandons the assumption of normality of data in the original regression, and replaces it with an assumption of normality in the logarithmic regression. As already remarked, there is no a priori evidence to suggest that we are dealing with a normal distribution in either the original or the transformed dependent variable.

Model variables may be sequentially included or deleted in either form of the model, and the effects on goodness of fit compared including or excluding any variable. Although the program permits up to 20 regression coefficients to be simultaneously determined, it is desirable in practice to hold the number to ten or less in order to have sufficient statistical strength to determine them from the available data.

C. Logit models

Logit models are usually applied to situations where the observations of dependent variables are dichotomous (e.g., in the present study, disease can be considered as present at a site or not present there; more generally, qualitative variables can be arbitrarily assigned numerical values for the purposes of labeling). From given data at a set of sites, the probability of disease occurrence for any given new values of the independent

variables is then sought. Since we deal from the outset with probabilities, the possibility of negative disease incidence rates is completely eliminated.

The general form of the model that was used on this project is as follows:

Let P(k,1) be the probability that a disease site k belongs to the class 1. In this case, class 1 may be taken as the case in which disease is recorded at the site. Similarly, let P(k,2) be the probability that site k belong to the class 2, where disease does not occur. Then the assumed form of the model that relates the probabilities P(k,i) to the independent variables L(j,k) is:

$$P(k,i) = \exp\left(\sum_n a(n,i).L(n,k)\right) / \left\{ \exp\left(\sum_n a(n,1).L(n,k)\right) + \exp\left(\sum_n a(n,2).L(n,k)\right) \right.$$

------(4)

It follows at once that

$$\ln(P(k,1)/P(k,2)) = \sum_n (a(n,1) - a(n,2)).L(n,k) \qquad \text{------(5)}$$

Since it is only the difference (a(n,1) - a(n,2)) that enters the equations (5), a(n,2) can be chosen as zero without loss of generality, and we have the single set of equations from which to determine a(n,1):

$$\ln(P(k,1)/P(k,2)) = \sum_n a(n,1).L(n,k) \qquad \text{------(6)}$$

which closely resembles equation (3) for the linear regression model.

Having determined the coefficient set a(n,1), the predicted disease incidence rates for any set of the independent variables L(n,k) is given by:

$$P(k,1) = F/(1 + F) \qquad \text{------(7)}$$

$$\text{where } F = \exp\left(\sum_{n} a(n,1).L(n,k)\right) \qquad \text{------(8)}$$

and of course $P(k,2) = 1 - P(k,1)$.

The logit model can be shown to be distribution independent,[21] and it is known to be a robust method of estimation. Its weakness in the present context is that it is designed to accommodate situations where the observed disease incidence rates extend over the full range from 0 to 1. For full efficiency, all rates should be possible in the data, from no cases observed, to the complete infection of every person at a disease observation site. In practice, the observed rates per 100,000 never exceed 100. Thus only a small part of the full range of available probabilities is sampled by the given data.

As in the case of the linear regression model, up to 20 different coefficients may be solved for simultaneously; in practice, it is desirable to keep that number to less than ten with the limited number of test sites available for this project.

Since the logit models were originally developed to study dichotomous variables, they also offer a possible technique for performing discriminant analysis. They were not employed in that way on this project.

D. Discriminant analysis

The discriminant analysis performed on this project was based upon a maximum likelihood classifier. The general assumptions that underlie the classification of Landsat data are as follows:

1. The spectral reflectances (grey levels) at each picture element can be used to assign every picture element to some group, or class, of picture elements.

2. These classes can be defined either in terms of representative ground areas chosen by a human interpreter (this is termed supervised classification) or by the natural clustering of data points in the space of spectral reflectances (unsupervised classification). In either case, the classes are assumed to be sufficiently well-separated that assignment of picture elements to classes on a probabilistic basis has significance.

3. When the classes have been defined in some region of a Landsat image, picture elements elsewhere in the image can be assigned to the appropriate class. The assignment will be unambiguous for most picture elements.

Once the image has been classified, the region about each disease incidence site can be categorized in terms of the mixture of classes present within it. The class proportions can then be correlated with observed disease incidence rates using a regression model.

Alternatively the classes themselves can be defined in the supervised classification mode by requiring that the classes are in one-to-one correspondence with ranges of disease incidence as observed at the disease sites.

To see how this works, suppose that we associate a ground area A with a disease site. Suppose that A contains within it N picture elements, and the disease site has an observed disease incidence rate of R per 100,000. We consider all sites with the same disease incidence rate R, and regard the picture elements contained within all such sites as a single data set. The spectral reflectances of the picture elements in this combined data set are used to define one group in spectral reflectance space, which we term the class associated with disease incidence rate R.

Each disease incidence rate is used to define a set of associated ground areas, and hence to define a class. In practice, the disease rates are grouped into ranges, to reduce the number of classes to some number of the order of ten. Any picture element in the whole image can now be assigned to a disease incidence rate, by determining to which class it belongs.

The problem with this approach is the assumption that the disease incidence rates will allow the definition of non-overlapping classes. If the defined classes are such that there is no clear separation of one from another in spectral reflectance space, the assignment of any new picture element is correspondingly difficult. A picture element may appear to belong to no defined class, or to several classes.

The discussion here has been in terms of the Landsat spectral reflectances, but it can be applied to any other physical variables by associating their values with each picture element and treating them in just the same way as the spectral reflectances.

V. DATA PROCESSING PROCEDURES

A. The Landsat data base

Landsat coverage of all of Taiwan except the extreme northern and southern tips of the island is provided by a pair of Landsat frames. To create the necessary Landsat data base, frames 1101-01550 and 1101-01552, imaged by the satellite on November 1, 1972, were combined in the computer to yield a single continuous image (see Report Cover) which contains a total of approximately 12,000,000 picture elements. The imaged area is almost cloud-free except in the central mountainous region. There is, however, a light fog or haze along most of the western coastal plain, including much of the land area where disease sites are located. The fog is most visible in the shortest wavelength band, and shows progressively less visible in the longer wavelength bands.

The fog may lead to two possible and opposite effects on image classification:

1. Classification resolution may decrease because image resolution is decreased; or

2. Fog density may correlate well with general humidity, which is a potentially significant variable for incidence of disease; the presence of haze may therefore improve the disease/Landsat correlations.

Before using Landsat data in the disease distribution models, two types of radiometric corrections were applied. The first of these, termed scan line suppression, corrects for the miscalibration of different on-board detectors in the Multi-Spectral Scanner. An uncorrected image shows

a characteristic six-line banding pattern, which will degrade the statistics of the models. In addition to the overall detector miscalibration, the Taiwan images also contained occasional partial lines of missing data. In such cases, data values were provided by linear interpolation from the nearest neighbor lines of picture elements. This correction provided images improved in appearance and probably made little difference to the computed model results since in all cases examined by eye the dropped data lines were seen only in offshore areas.

The disease incidences were provided as point data, i.e., each was given at a single latitude and longitude. It is unrealistic to treat them as point data in the model for several reasons. First, the disease site data represent disease statistics collected for some defined region (a village or township) on the ground. Second, in converting latitudes and longitudes to coordinates on the image, there is a probable error of at least a few tens of metres, and often a hundred metres or more, in relating the two different coordinate systems. Third, whatever the geographic variables may be that control the incidence and spread of the disease, they are probably spread over several hundred metres on the ground, since the vector is mobile over such a range. Fourth, the accuracy of the original disease site locations is unknown. It is therefore logical to associate some group of picture elements with each disease site, of a size to be determined by experiments with the model.

The fourth point above was confirmed when the given disease site locations were plotted on the Landsat images and on 1:50,000 scale topographic

maps of the island. Every site was found to be very close to, but rarely coincident with, a visible town or village. It was concluded that the towns and villages were intended as the disease sites, but that the latitudes and longitudes provided had been rounded in value. Adjustments to the given site locations were therefore made, so as to center them on the corresponding urban area.

At this point, a new consideration appeared. Clearly, disease data were collected where people are present. Equally clearly, where people are present there will be signs of habitation visible on the image data base. Thus, the strongest likely correlation between disease data and image data would be one that associated disease with visible signs of human habitation. However, since the objective of the project is the prediction of disease-prone areas in regions that may lack any current urban patterns, correlation with present human activities is not useful. It is therefore necessary to find a technique that correlates disease occurrence with <u>natural</u> geographic variables, and not simply with the existence of towns and villages.

This point should be explored a little further. It is certainly true that villages are likely to be foci for disease occurrence, and that the number of cases per 100,000 will probably be higher there than in rural parts, since the vector can readily proceed from one host to the next. However, it is also likely that ground disturbances introduced by human activity, such as for example the creation of paddies and ponds, will also serve to increase the probability of disease occurrence. It is desirable to be able to dissociate these two factors. The logic used to perform that dissociation is based upon the fact that the ground disturbances produced by human agricultural

activity extend well beyond the main towns and villages. If areas of the Landsat data base are selected that are centered on the visible urban disease site locations but that exclude the urban development itself, correlation of the disease with such areas will reflect dependence on geography, but not on the visible urban development.

To create the data base needed for the model, sets of "windows" were therefore selected from the Landsat data. Each window consisted of a square array of picture elements, with central picture element at a given disease site. Two different types of windows were used in the models. The first was a full array, usually 10x10, which therefore included the central urban development visible on the image; the second was an array of size 14x14, with the central 10x10 array of picture elements, and hence the associated urban area, excluded. Model runs were performed using both "full" and "hollow" windows. The hollow window occupies almost the same ground area (96 picture elements, or 107 acres) as the full window (100 picture elements, or 111 acres). See Figure 4.

B. Weather data

Previous work on the etiology of Japanese encephalitis suggests that in addition to possible correlation with geographic variables there may be a relationship with climatic variables. Local rainfall, temperature, and humidity may all be factors in the occurrence and spread of JE.

With this in mind, weather station locations were obtained for Taiwan, and their positions noted in relation to the disease sites. Only thirteen stations are present in the island (see Table 1) and it is clear that they

FIGURE 4. Landsat picture element arrays associated with disease sites.

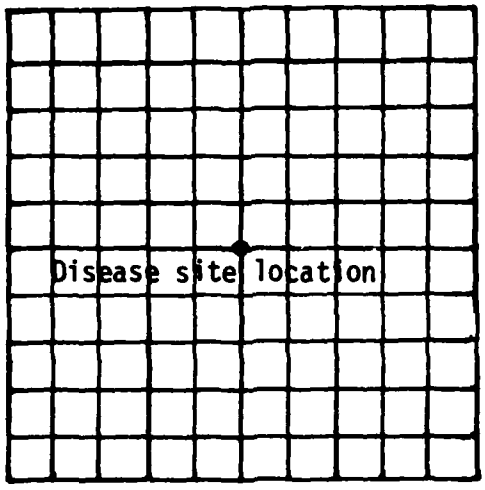

Full Array, 10x10

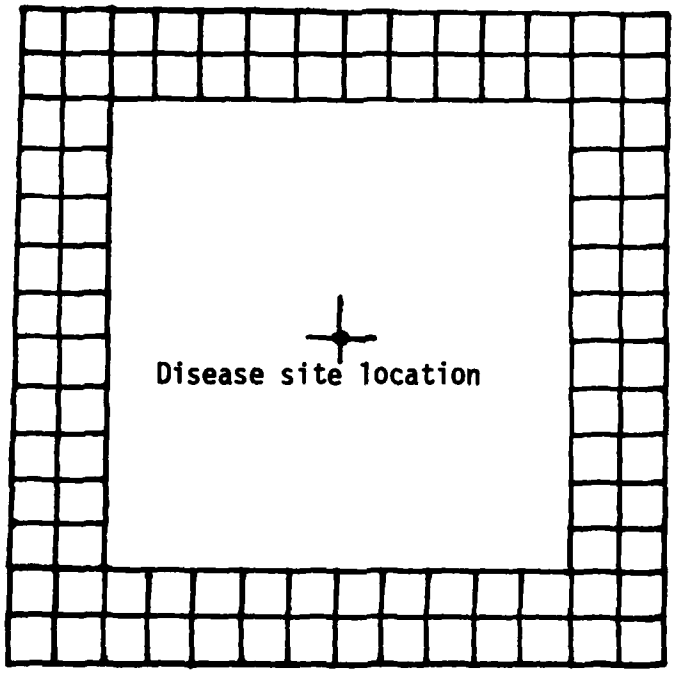

Hollow Array, 14x14 with excluded 10x10 center

TABLE 1

WEATHER STATION NAME	LOCATION LATITUDE / LONGITUDE	
Kao-Hsiung	22° 34' N	120° 20' E
Ping Tung South	22° 40' N	120° 27' E
Taitung	22° 45' N	121° 09' E
Tainan	22° 57' N	120° 12' E
Chia-I	23° 27' N	120° 22' E
Ali-Shaw	23° 28' N	120° 52' E
Taiwu	23° 34' N	119° 37' E
Hua-Lien	24° 01' N	121° 36' E
Taichung	24° 11' N	120° 38' E
Kinmen	24° 25' N	118° 20' E
Hsin-Chu	24° 49' N	120° 56' E
Taipei	25° 04' N	121° 32' E
Matsu	26° 10' N	119° 56' E

are much too few in number and widely separated in location to contribute to the highly localized variations in disease occurrence. Weather data could not therefore contribute significantly to the model, and were omitted from the analysis. It is still likely that local weather data, if available, would significantly improve the disease distribution model.

C. Altitude data and location data

The height above sea level of each disease site is available from 1:50,000 scale topographic maps of the island. Although most population centers and disease sites lie in the western coastal plain and have altitudes below 100 metres, the eastern sites lie on higher ground, up to 400 metres.

Altitude is a potentially important variable since it correlates directly and strongly with temperature and more weakly with humidity and wind speed, all of which can affect the abundance and distribution of the vector. The height above sea level was therefore determined from the topographic maps and included as an additional independent variable. However, since the altitudes show a strong east-west variation, it is possible that any observed correlation of disease with altitude indicates dependence not truly on altitude but on some other variable that also shows east-west differences, such as the on-shore or off-shore direction of prevailing winds. To test that hypothesis, a dichotomous variable with values 0 and 1 for eastern and western site locations was introduced as an alternative to height above sea level. Both these models were run and results compared.

D. Determination of the set of independent variables

Independent variables such as altitude or location are entered into the models directly, as continuous or discrete values. In the case of

the Landsat data, however, this is not possible. The set of 100 picture elements that comprises a window at one disease site provides 400 reflectance values (values in four spectral bands for every picture element). An attempt to use these values as independent variables would certainly fail, since reflectances are highly correlated with each other. There would in addition be more model coefficients than observations, which also guarantees a singular set of regression equations. It is therefore necessary to derive from the 400 reflectances at a disease site some smaller set of aggregate values to use as independent variables.

Since reflectance values at any site, k, are highly correlated, most of their local variability can be expressed through their first and second moments, i.e., through the use of the mean reflectance in each band i, M(i,k), the variance of reflectance in each band, S(i,k), and the covariance between bands, C(i,j,k). This yields a model with 14 independent variables derived from Landsat data (4 means, 4 variances, and 6 covariances since C(i,j,k) = C(j,i,k)), of the form:

Disease incidence at site k =

$$a + \sum_{i=1}^{4} \{m(i).M(i,k) + s(i).S(i,k)\} + \sum_{i=1}^{4} \sum_{j<i} c(i,j).C(i,j,k) \quad \text{------(9)}$$

where a, m(i), s(i) and c(i,j) are to be determined from the observed disease data. (Note: For brevity we quote only the regression form of models in this section; analogous forms exist for the logit and discriminant analysis models.)

In practice, there is high correlation between the different bands of Landsat data. It is therefore logical to develop the variance-covariance matrix

for the whole set of picture elements associated with all disease locations, to diagonalize this, and to use just the variances, D(i,k), of the diagonalized system in the model in place of the original variances and covariances. This reduces the number of Landsat-derived independent variables to 8, and yields a regression model of the form:

Disease incidence at site k =

$$a + \sum_{i=1}^{4} (m(i).M(i,k) + d(i).D(i,k)) \qquad \text{------(10)}$$

Use of the form (10) implies that the transformations used to diagonalize the covariance matrix for the whole set of disease sites will approximate those transformations that diagonalize the covariance matrix at each disease site. The only practical test of this assumption is the success or failure of this form of the model given in (10).

In addition to the independent variables derived from Landsat data, the models include the altitude variable H(k) and/or the dichotomous east-west location variables, P(k). This gives the most general final form used for the regression model:

Disease incidence at site k =

$$a + \sum_{i=1}^{4} \{m(i).M(i,k) + s(i).S(i,k)\} + \sum_{i=1}^{4} \sum_{j<i} c(i,j).C(i,j,k)$$

$$+ h.H(k) + p.P(k) \qquad \text{------(11)}$$

to determine the coefficients a, h, p, m(i), s(i), and c(i,j).

VI. RESULTS OF THE STATISTICAL MODELS

A. General comparison of the logit and regression models

The first model comparisons were made on a set of 44 disease sites in south Taiwan, using filled square windows containing 100 picture elements in each. Computer runs were performed for the linear regression models and the logit models, first with the means and unrotated variances of equation (9), then with the means, unrotated variances and covariances of equation (9), and finally with the means and rotated variances of equation (10). Since the filled windows include urban areas on the image, correlations will be expected between density of urban development and disease occurrences. The first group of tests was therefore regarded as providing information concerning the preferred models and the number and type of parameters that should be used in each model, rather than offering final "best sets" of coefficients for any model.

The first conclusion was that the logit model, while displaying a goodness-of-fit result that suggests the model is statistically valid, was not suitable to the problem, largely because the disease occurrence ratios are so small (from 0 to 0.001). As observed in Section IV.A, the logit models are designed to handle cases in which the dependent variable takes on the full range from 0 to 1.

In an attempt to remedy the situation, disease incidence rates per 100,000 were scaled by empirically chosen factors ranging from 10 to 400. The results of two model runs in which the means and unrotated variances of the Landsat data were used as independent variables are shown in Tables 2 and 3. Even with the best choice of scaling factor, the results using

TABLE 2. Logit model, 9 independent variables, scaling factor = 10.

	NON-DISEASE PROPORTIONS		
	OBSERVED	PREDICTED	ERROR
1	0.995	0.980	0.015
2	0.994	0.995	-0.001
3	1.000	0.994	0.006
4	0.993	0.995	-0.002
5	0.988	0.990	-0.001
6	1.000	0.994	0.006
7	0.992	0.992	0.001
8	0.997	0.995	0.003
9	1.000	0.997	0.003
10	1.000	0.991	0.009
11	1.000	0.992	0.008
12	1.000	0.989	0.011
13	0.998	0.996	0.002
14	0.997	0.996	0.002
15	1.000	0.992	0.008
16	1.000	0.994	0.006
17	1.000	0.995	0.005
18	0.953	0.954	-0.001
19	0.986	0.995	-0.009
20	0.977	0.993	-0.016
21	1.000	0.994	0.006
22	0.979	0.994	-0.015
23	0.971	0.990	-0.018
24	0.965	0.978	-0.012
25	0.998	0.995	0.002
26	0.996	0.995	0.000
27	1.000	0.995	0.005
28	0.994	0.992	0.002
29	1.000	0.994	0.006
30	0.995	0.994	0.000
31	0.997	0.995	0.003
32	0.996	0.995	0.002
33	1.000	0.994	0.006
34	0.991	0.995	-0.003
35	0.989	0.994	-0.005
36	1.000	0.995	0.005
37	0.997	0.994	0.003
38	0.996	0.995	0.001
39	0.983	0.996	-0.012
40	1.000	0.995	0.005
41	1.000	0.995	0.005
42	1.000	0.995	0.005
43	0.995	0.995	-0.000
44	0.995	0.991	0.004

TABLE 3. Logit model, 9 independent variables, scaling factor = 400

	NON-DISEASE PROPORTIONS		
	OBSERVED	PREDICTED	ERROR
1	0.840	0.557	0.283
2	0.797	0.865	-0.068
3	1.000	0.823	0.177
4	0.771	0.860	-0.089
5	0.681	0.752	-0.071
6	1.000	0.826	0.174
7	0.765	0.764	0.001
8	0.903	0.847	0.056
9	1.000	0.911	0.089
10	1.000	0.738	0.262
11	1.000	0.780	0.220
12	1.000	0.710	0.290
13	0.918	0.883	0.036
14	0.905	0.894	0.011
15	1.000	0.766	0.234
16	1.000	0.854	0.146
17	1.000	0.866	0.134
18	0.337	0.347	-0.010
19	0.632	0.847	-0.215
20	0.518	0.801	-0.283
21	1.000	0.838	0.162
22	0.538	0.844	-0.306
23	0.458	0.724	-0.267
24	0.408	0.525	-0.117
25	0.911	0.887	0.024
26	0.849	0.883	-0.035
27	1.000	0.874	0.126
28	0.810	0.773	0.037
29	1.000	0.837	0.163
30	0.820	0.841	-0.022
31	0.909	0.851	0.057
32	0.871	0.850	0.021
33	1.000	0.850	0.150
34	0.737	0.856	-0.119
35	0.699	0.840	-0.141
36	1.000	0.876	0.124
37	0.895	0.847	0.048
38	0.849	0.852	-0.003
39	0.595	0.878	-0.283
40	1.000	0.862	0.138
41	1.000	0.872	0.128
42	1.000	0.869	0.131
43	0.835	0.863	-0.028
44	0.840	0.765	0.075
R.M.S. ERROR			0.155

the logit models were still observed to be generally inferior to those of the regression models. In later experiments, attention was therefore focussed on the latter.

A second conclusion, borne out in both the logit and regression model runs, is that the inclusion of Landsat data covariances decreased the statistical strength of the results. This indicates that the cross-correlation terms allow the models to account for an increased amount of total observational variance, but only at the expense of overfitting the data. The most successful results were actually obtained using the means and the unrotated variances of the Landsat data. In later model runs, attention was therefore focussed on the use of means and unrotated variances only, plus non-Landsat variables as described below.

B. General results of the discriminant analysis

Using a maximum likelihood classifier and a total of 44 data points, 22 windows were randomly selected as training sites for the discriminant analysis, and the remaining 22 sites were reserved as model test sites. The disease incidence rates were divided into ten ranges, from zero disease rate to maximum observed disease rate, and each of the 22 windows of the training sites was assigned to the appropriate disease range based upon the given disease incidence rate. The ten disease ranges were then regarded as defining ten classes, to which any disease site could be assigned, and a maximum likelihood classifier was run to determine the statistical characteristics of the ten classes.

Each of the 22 test sites was then assigned using the classifier. The assigned class was then compared with the observed class based on the actual disease rate.

The results obtained were as follows (this is the average obtained from six different runs and assignments of class range):

Test sites classified correctly: 3

Test sites classified with error of one range: 5

Test sites classified with error of two ranges: 2

Test sites classified with error of three ranges: 4

Test sites classified with error of four ranges: 1

Test sites classified with error of five ranges: 2

Test sites classified with error of six ranges: 3

Test sites classified with error of seven ranges: 0

Test sites classified with error of eight ranges: 2 TOTAL: 22 sites

On a purely random basis, if there were no correlation at all between training site and test site ranges, the average error in test site ranges would be 3.3 units. The observed error in test site ranges had an average of 3.14. This is consistent with a random classification result. The discriminant analysis model was therefore judged unsatisfactory for this application. A second series of tests, employing 63 disease sites, gave similar results.

To summarize these findings, the discriminant analysis techniques proved unable to define "clean" classes of Landsat data that corresponded to disease incidence. Classes contained widely scattered data points, and assignment of

a data point to a particular class was ambiguous. This is probably due to the degree of variability of Landsat data, considered on an individual picture element-by-picture element basis. The averaging over many Landsat picture elements employed in the logit and regression models thus appear central to the development of a successful model.

C. Results of the regression models and the addition of other variables

All the computer runs described in VI.A and B used Landsat variables alone as independent variables. Based on those results, it was decided to focus on regression models for subsequent experiments with the data.

1. Results comparing different independent variables drawn from Landsat data

Initial runs of the regression model, as already noted, employed data from 44 disease sites in southern Taiwan, and a filled 10x10 array of Landsat picture elements centered at disease sites. Runs were performed using means and unrotated variances only; means, variances and covariances; and means and rotated variances.

The results were as follows:

a. Means and unrotated variances: $R^2 = 0.42$

b. Means, variances and covariances: $R^2 = 0.35$

c. Means and rotated variances: $R^2 = 0.38$

This indicates that inclusion of the covariances over-fits the data, and that use of the rotated variances for the whole data set degrades the results, presumably because the rotations that are suitable for the whole set of picture element arrays are not suitable for the arrays considered separately.

2. Results using filled versus hollow arrays

It had been observed in early runs of the regression model that worse fits were obtained if the array centers did not quite correspond to the disease site location. It was this observation that led to a suspicion that the main correlations obtained were with visible urban development, rather than natural geographic variables. This led in turn to the use of hollow arrays of picture elements that would exclude the central urban area associated with a disease site.

Using the regression model with a 10x10 full window and then a 14x14 hollow window, the results were as follows (the data base was again a set of 44 disease sites in southern Taiwan):

a. Filled window: $R^2 = 0.42$

b. Hollow window: $R^2 = 0.37$

Using a set of 57 disease sites, in northern and southern Taiwan, the corresponding results were:

a. Filled windows: $R^2 = 0.42$

b. Hollow windows: $R^2 = 0.39$

The exact equality of R^2 (to 2 significant figures) for the filled window results is no more than coincidental, since the individual residuals at particular disease sites show no particular pattern. However, the higher value of R^2 obtained with filled windows confirmed the conjecture that the correlation was partly with urban features, rather than with natural geographic variables. With the hollow windows, there is weak positive correlation (the correlation coefficient ranged from 0.61 to 0.65 in different model runs). In

view of the fact that it is correlations with natural geography that are sought, rather than relation of disease to urban developments, hollow windows were used throughout the remaining model runs, despite the rather lower correlations that this produced in the above tests.

3. Results including other variables

Using data from 44 disease sites in southern Taiwan, and hollow 14x14 arrays at each site, altitude was now added as an independent variable. In a second series of runs on the same data, east/west location was added as a dichotomous variable. Finally, runs were performed using altitude alone, in order to explore the extent to which this might account for all significant correlation with disease incidence.

The results obtained are as follows:

a. Landsat data alone: $R^2 = 0.37$

b. Landsat data plus altitude: $R^2 = 0.57$

c. Landsat data plus east/west position: $R^2 = 0.40$

d. Altitude data alone: $R^2 = 0.41$

The individual residuals showed no particular pattern.

D. Other experiments and the summary of results

A complete testing of all models would require computer runs with all available data sets, with filled and hollow windows, with rotated and unrotated variances, and with altitude and east/west location included and excluded. Consideration of all such combinations would lead to an

impossibly high number of computer runs. The sequential method described in the previous three sections was therefore employed, in which only the best model at each stage was used in subsequent experiments.

This procedure can be criticized as too restrictive, since there is always the possibility that a model rejected early on the basis of a set of experiments would prove superior when other variations were later performed. To provide a limited test of this, additional model runs were performed using the 44 site data set, altitude data, and hollow array windows. As a separate check on the discriminant analysis approach, the logit classifier was used as a non-parametric maximum-likelihood classifier.

The results of these runs supported those of Section VI.C, i.e., the regression model gave better results than either the logit model or the discriminant analysis, and altitude information plus Landsat data gave stronger correlations than any other combination of variables. The runs with filled arrays continued to give higher correlation than those with hollow arrays, but the suspicion that this is due mainly to correlation with urban land use remains.

The overall results of all experiments can therefore be summarized as follows:

1. Of the types of models employed on the project, regression models proved superior to either logit models or discriminant models.

2. A regression model with 9 independent variables provided the best correlations with the disease data.

3. Hollow arrays of Landsat data surrounding each disease incidence site were judged necessary, to eliminate the effects of urban development on computed correlations.

4. The best combination of variables consists of Landsat-derived variables (means and variances) plus altitude.

5. Using the best model, a value of $R^2 = 0.57$ (correlation coefficient = 0.75) was obtained. This is statistically significant.

6. Varying the input data to include different numbers and locations of disease test sites produced only small effects on the computed results (R^2 ranged from 0.51 with only 15 sites, to 0.56 with 63 sites). The model thus appears insensitive to the particular choice of sites, either in number or placement.

7. No systematic bias could be observed in computed results, and the residuals at disease sites appear to be uncorrelated with location, altitude, or degree of urban development. Possible correlation of residuals with temperature, humidity, and precipitation is still unknown.

VII. CONCLUSIONS

The objective of this study was to explore statistical relationships between geographic variables, principally those obtained by the Landsat satellite systems, and the observed occurrence of Japanese encephalitis on Taiwan. To accomplish this end, Landsat data, location data (latitude and longitude) and altitude data were employed to develop four different types of statistical model, namely, linear regressions, log-linear regressions, logit models, and discriminant analyses. Observed disease incidence for the period 1968-1975, for 106 sites in Taiwan, constituted the dependent variable.

Landsat data were used in the form of the means, variances and covariances associated with surface reflectance for groups of picture elements centered on disease incidence locations. Both unrotated and rotated (principal component) variances were employed in the models.

Following a substantial series of experimental computer runs, it was concluded that the linear regression models give the best results of the four models considered. In particular, the preferred model is a 9-variable linear regression, employing as independent variables Landsat means and unrotated variances (drawn from 96-pixel hollow windows surrounding each disease incidence site), together with altitudes. With this model a statistically significant correlation (correlation coefficient 0.75) is obtained between the observed and predicted disease incidences.

Computer runs performed using different data sets suggest that the results are insensitive to the number and position of disease sites used to determine the model coefficients. In addition, the residuals (the difference of observed and computed values) display no systematic bias in terms of

location, altitude, or other geographic variable. The technique therefore shows promise as a predictive tool for geographic areas where disease data are lacking, or of doubtful quality.

Although the results described are specific to the single disease of Japanese encephalitis in a particular location, the methods used and programs developed are quite general. The form of model and data manipulations should be applicable to infectious diseases with airborne insect vectors, in any location.

The study was conducted under a number of significant constraints, and stronger results may be obtained if one or more of them could be relaxed. The most important constraint is probably the fact that the Landsat data base was drawn from a single date (November 1, 1972). The information revealed by Landsat certainly changes significantly with season, and has substantial year-by-year variations. Additional constraints were provided by the absence of suitably detailed weather data, by the uncertain quality of the disease incidence data, and by a practical limitation on the number of different window sizes and statistical techniques that could be employed.

Given these restrictions, the positive correlations observed between disease incidence and Landsat observables is encouraging, and perhaps even surprising. It would be natural for disease occurrence to correlate with urbanization, but since urban centers were excluded by the use of hollow windows, the correlation is almost certainly due to a real relationship between geographic variables (which may include human agricultural practices) and disease occurrence.

The distribution model developed here is no more than a beginning. Additional effort is needed to confirm present results using satellite data of different dates; to extend the model geographically, ideally to other countries and to different topographic and climatic environments; and to explore through biological and geographic analysis the reasons for Landsat's positive correlation with observed disease. Beyond this, it is natural to consider application to other diseases, with other airborne or waterborne vectors.

In all cases, the satellite data base is already available, and use of weather satellites in addition to Landsat may permit the inclusion of climatic variables to supplement ground weather station information. The limiting factor on future investigations will probably be the availability of suitable disease data.

REFERENCES

1. G. Fracastoro, "De Contagionibus et Contagiosis Morbis et Eorum Curatione" (On Contagion, Contagious Diseases, and Their Cure); 1546, tr. W. C. Wright, Putnam's, 1930.

2. L. Pasteur "Etudes sur les maladies des vers a soie" (1870).

3. R. Koch "Die Aetiologie der Tuberculose" (The Aetiology of Tuberculosis); 1882, tr. M. Pinner, Am. Rev. Tuber., March,1932.

4. Theobald Smith & F. L. Kilborne, "Investigations into the Nature, Causation and Prevention of Southern Cattle Fever"; Bureau of Animal Industry, 1893.

5. Walter Reed, "The Propagation of Yellow Fever; Observations Based on Recent Researches" Med. Rec. 60, No. 6, August 1901.

6. W. A. Fischer et al., "History of Remote Sensing"; in Manual of Remote Sensing, ed. R. G. Reeves, pp. 27-29; American Society of Photogrammetry, Falls Church, Virginia (1975).

7. Ibid., pp. 31-34.

8. Ibid., pp. 35-36 and 40-41.

9. Principal Investigators, Earth Resources Technology Satellite-A. Goddard Space Flight Center report (undated; the Principal Investigator agreements listed were those signed as of June 21, 1972).

10. G. Arp et al., "System Development of the Screwworm Eradication Data System"; Johnson Space Center Technical Memorandum JSC-10965 (1976).

11. C. Sheffield, "Earth Resources and Satellite Imaging Systems"; Interdisciplinary Science Reviews, Volume 7, Number 2, Heyden, London (1982).

12. J. T. Grayston, San-Pin Wang, and Chun-hui Yen, "Encephalitis on Taiwan, I: Introduction and Epidemiology"; American Journal of Tropical Medicine and Hygiene, Vol. II, No. 1, pp. 126-161 (1962).

13. T. S. Hsu, C. T. Huang, and S. T. Hsu, "Epidemiology and Control of Japanese Encephalitis in Taiwan"; Japan Journal of Tropical Medicine, Vol. 10, pp. 165-174 (1969).

14. S. M. Wang, "Japanese Encephalitis on Taiwan"; United States Medical Research Unit, Lecture and Review Series, Report No. 62-4 (1962).

15. H. S. Hurlbut, "The Ecology of Japanese Encephalitis Virus"; United States Medical Research Unit, Lecture and Review Series, Report No. 63-2 (1983).

16. W. K. Reisen, M. Aslamkhan, and R. G. Basio, "The effects of climatic patterns and agricultural practices on the population dynamics of Culex Tritaeniorhynchus in Asia"; Southeast Asia Journal of Tropical Medicine, Vol. 7, No. 1 (1976).

17. G. W. Snedecor and W. G. Cochran, Statistical Methods; Chapter 6, Sixth Edition, Iowa State University Press (1972).

18. Ibid, Chapter 13.

19. R. D. Bock, "Estimating Multinomial Response Relations"; Essays in Probability and Statistics, Chapter 6, ed. R. C. Bose (1967).

20. R. B. Erb, "An overview of the large area crop inventory experiment and the outlook for a satellite crop inventory"; Johnson Space Center Report JSC-13761 (1979).

21. N. E. Day and D. F. Kerridge, "A general maximum likelihood discriminant"; Biometrics 23, pp. 313-323 (1967).

APPENDIX A: DISEASE STATISTICS

LOCATION	LATITUDE/LONGITUDE	DISEASE RATE PER 100,000	NUMBER OF CASES	POPULATION
Chia-I	23.29 N 120.27 E	4.8	12	252,037
P'o-Tzu	23.28 N 120.14 E	6.4	3	47,142
Pu-Tai	23.23 N 120.09 E	0	0	42,419
Ta-Lin	23.36 N 120.27 E	7.4	3	40,357
Min-Hsiung	23.33 N 120.25 E	11.7	6	51,254
Hsi-K'ou	23.36 N 120.23 E	0	0	21,665
Hsin-Kang	23.34 N 120.20 E	7.7	3	39,137
Liuchiao	23.30 N 120.15 E	2.7	1	37,277
Tung-Shih	23.28 N 120.08 E	0	0	39,896
I-Chu	23.20 N 120.14 E	0	0	30,375
Lu-Ts'ao	23.25 N 120.17 E	0	0	23,130
T'ai-Pao	23.28 N 120.19 E	0	0	26,929
Shui-Shang	23.26 N 120.23 E	2.2	1	45,062
Chung-Pu	23.25 N 120.31 E	2.6	1	37,988
Chu-Chi	23.31 N 120.32 E	0	0	41,931
Mei-Shan	23.35 N 120.33 E	0	0	25,680
Fan-Lu	23.27 N 120.33 E	0	0	13,134
Ta-Pu	23.18 N 120.35 E	49.1	2	4,071
Hsin-Chu	24.48 N 120.58 E	18.7	45	240,900
Kuan-Hsi	24.48 N 121.10 E	37.0	14	37,837
Hsin-Pu	24.49 N 121.04 E	19.8	7	35,394
Chu-Tung	24.44 N 121.05 E	23.0	16	69,676
Hsiang-Shan	24.46 N 120.54 E	17.3	7	40,471
Chu-Pai	24.50 N 121.00 E	21.5	12	55,819

LOCATION	LATITUDE/LONGITUDE	DISEASE RATE PER 100,000	NUMBER OF CASES	POPULATION
Hu-Kou	24.54 N 121.02 E	34.5	16	46,342
Hsin Chuangtzu	24.43 N 121.06 E	40.5	8	19,736
Hsin Ch'eng	24.46 N 121.09 E	6.4	2	31,180
Hsiunglin	24.47 N 121.04 E	0	0	18,227
Pao-Shan-Tsun	24.44 N 121.01 E	8.3	1	12,019
Pei-Pu	24.42 N 121.03 E	8.5	1	11,738
O-Mei	24.41 N 121.01 E	98.1	8	8,153
Chien-Shih	24.43 N 121.13 E	33.2	3	9,043
Wufeng	24.37 N 121.06 E	0	0	5,402
Miao-Li	24.33 N 120.49 E	7.4	6	81,207
Yuang-Li	24.27 N 120.39 E	2.0	1	49,311
T'Ung-Hsiao	24.29 N 120.40 E	4.5	2	44,585
Chu-Nan	24.41 N 120.52 E	1.8	1	54,546
T'ou-Fen	24.41 N 120.54 E	27.1	18	66,491
Hou-Lung	24.37 N 120.47 E	36.4	17	46,680
Cho-Lan	24.19 N 120.49 E	78.0	16	20,521
Ta-Hu	24.25 N 120.51 E	4.6	1	21,949
Kung-Kuan	24.30 N 120.49 E	15.2	5	32,963
T'ung-Lo	24.29 N 120.47 E	26.8	6	22,354
Nan-Chuang	24.36 N 120.59 E	15.0	3	20,043
T'ou-Wu	24.34 N 120.50 E	23.8	3	12,600
Tsao-Ch'iao	24.38 N 120.51 E	14.0	2	14,256
San-Wan	24.39 N 120.57 E	63.2	7	11,076

LOCATION	LATITUDE/LONGITUDE	DISEASE RATE PER 100,000	NUMBER OF CASES	POPULATION
Shih-T'an	24.32 N 120.55 E	34.4	3	8,710
Hua-Lien	23.58 N 121.36 E	7.8	8	102,665
Feng-Lin	23.43 N 121.26 E	15.1	3	19,857
Yu-Li	23.20 N 121.18 E	14.6	6	41,225
Hsin-Ch'eng	24.08 N 121.39 E	11.4	2	17,510
Chi-An	23.58 N 121.33 E	30.8	15	48,771
Shou-Feng	23.52 N 121.30 E	23.6	6	25,398
Kuang-Fu	23.23 N 121.19 E	23.2	5	21,519
Feng-Pien Ts'un	23.36 N 121.31 E	0	0	8,699
Jui-Sui	23.30 N 121.22 E	21.5	4	18,603
Fu-Li Ts'un	23.10 N 121.14 E	29.6	6	20,263
Hsiulin	24.07 N 121.37 E	27.7	4	14,430
Cho-Hsi Ts'un	23.21 N 121.17 E	36.3	3	8,274
Chang-Hua	24.05 N 120.32 E	10.0	18	181,359
Lu-Kang	24.03 N 120.25 E	16.6	12	72,474
Ho-Mei	24.06 N 120.29 E	12.2	8	65,337
Pei-Tou	23.52 N 120.31 E	7.0	2	28,767
Yuan-Lin	23.57 N 120.34 E	4.9	5	102,554
Hsi-Hu	23.57 N 120.28 E	4.3	2	46,259
T'ien-Chung	23.52 N 120.35 E	0	0	45,374
Erh-Lin	23.54 N 120.21 E	1.7	1	59,579
Hsienhsi	24.08 N 120.27 E	0	0	15,000
Shen-Kang	24.09 N 120.28 E	18.8	5	26.649
Fushing	24.03 N 120.24 E	15.0	6	10,214

LOCATION	LATITUDE/LONGITUDE	DISEASE RATE PER 100,000	NUMBER OF CASES	POPULATION
Hsiushui	24.03 N 120.30 E	10.0	3	30,010
Huatan	24.02 N 120.32 E	8.2	3	36,653
Fenyuan	24.01 N 120.37 E	18.2	5	27,467
Tatsun	24.00 N 120.32 E	0	0	31,130
Pu-Yen Ts'un	23.59 N 120.28 E	5.9	2	33,815
P'u-Hsin	23.57 N 120.32 E	0	0	31,144
Yung-Ching	23.55 N 120.32 E	2.7	1	36,615
She-T'ou	23.54 N 120.35 E	0	0	39,828
Erh-Shui	23.49 N 120.36 E	0	0	22,545
Tienwei	23.54 N 120.30 E	0	0	29,130
Pitou	23.54 N 120.28 E	0	0	33,846
Fang-Wan	23.55 N 120.18 E	0	0	45,824
Ta-Ch'eng	23.52 N 120.19 E	3.6	1	27,443
Chu-T'ang	23.52 N 120.25 E	0	0	20,584
Chichou	23.51 N 120.29 E	0	0	36,838
Tun-Lin	23.42 N 120.31 E	2.4	2	81,651
Tou-Nan	23.41 N 120.28 E	4.6	2	44,895
Hu-Wei	23.43 N 120.25 E	0	0	66,570
Hsi-Lo	23.48 N 120.27 E	5.8	3	51,306
Tuku	23.41 N 120.23 E	0	0	35,724
Pei-Kang	23.34 N 120.17 E	5.5	3	54,552
Ku-K'eng	23.39 N 120.33 E	2.5	1	39,758
Tapi	23.39 N 120.25 E	3.7	1	27,020

LOCATION	LATITUDE/LONGITUDE	DISEASE RATE PER 100,000	NUMBER OF CASES	POPULATION
Tzutung	23.45 N 120.29 E	0	0	31,567
Lin-Nei	23.46 N 120.27 E	8.9	2	22,430
Erh-Lun	23.46 N 120.24 E	10.8	4	37,195
Lun-Pei	23.46 N 120.21 E	0	0	32,308
Mai-Liao	23.45 N 120.15 E	2.9	1	34,041
Tungshih	23.41 N 120.15 E	4.4	1	22,507
Pao-Chung	23.41 N 120.18 E	17.0	3	17,629
T'an-Hsi-Ts'un	23.38 N 120.16 E	0	0	35,350
Yuan-Ch'ang	23.39 N 120.18 E	0	0	39,142
Ssu-Hu	23.38 N 120.13 E	0	0	40,053
K'ou-Hu	23.35 N 120.10 E	4.9	2	40,526
Shu-Lin	23.54 N 120.14 E	4.8	2	42,052

OFFICE OF NAVAL RESEARCH
MICROBIOLOGY PROGRAM
STANDARD DISTRIBUTION LIST

Number of Copies:

(12)	Administrator, Defense Technical Information Center Cameron Station Alexandria, VA 22314
(6)	Director, Naval Research Laboratory Attn: Technical Information Division Code 2627 Washington, D.C. 20375
(3)	Office of Naval Research Department of the Navy Code 443 800 N. Quincy Street Arlington, VA 22217
(1)	Commanding Officer (Code 00) Naval Medical Research & Development Command National Naval Medical Center Bethesda, MD 20014
(1)	Naval Medical Research & Development Command Code 46 National Naval Medical Center Bethesda, MD 20014
(2)	Technical Reference Library Naval Medical Research Institute National Naval Medical Center Bethesda, MD 20014
(2)	Bureau of Medicine and Surgery Navy Department Code MED 314 Washington, D.C. 20372
(1)	Office of Naval Research Eastern/Central Regional Office Building 114, Section D 666 Summer Street Boston, MA 02210

STANDARD DISTRIBUTION LIST (Cont'd)

Number of Copies:

(1) Office of Naval Research Branch Office
536 South Clark Street
Chicago, IL 60605

(1) Office of Naval Research Western Regional Office
1030 East Green Street
Pasadena, CA 91106

(1) Commanding Officer
U.S. Naval Medical Research Unit #2
APO, San Francisco 96528

(1) Commanding Officer
U.S. Naval Medical Research Unit #3
FPO, New York 09527

(1) Officer in Charge
Submarine Medical Research Laboratory
U.S. Naval Submarine Base, New London
Groton, CT 06342

(1) Scientific Library
Naval Biosciences Laboratory
Naval Supply Center
Oakland, CA 94625

(1) Scientific Library
Naval Aerospace Medical Research Institute
Naval Aerospace Medical Center
Pensacola, FL 32512

(1) Commander, Naval Air Development Center
Attn: Code 6003
Warminster, PA 18974

(1) Commanding General
U.S. Army Medical Research & Development Command
Fort Detrick
Frederick, MD 21701
Attn: MEDDH-Sr

STANDARD DISTRIBUTION LIST (Cont'd)

Number of Copies:

(1) Director of Life Sciences
Air Force Office of Scientific Research
Bolling Air Force Base
Washington, D.C. 20032

(1) STIC-22
4301 Suitland Road
Washington, D.C. 20390

(1) Director
Walter Reed Army Institute of Research
Walter Reed Army Medical Center
Washington, D.C. 20012

END

FILMED

1-83

DTIC